# Au-$Cu_2O$ core-shell nanowire photovoltaics

S. Z. Oener, S. A. Mann, B. Sciacca, C. Sfiligoj, J. Hoang, and E. C. Garnett[a)]
*Center for Nanophotonics, FOM Institute AMOLF, Science Park 104, 1098 XG Amsterdam, The Netherlands*

(Received 22 October 2014; accepted 26 December 2014; published online 12 January 2015)

Semiconductor nanowires are among the most promising candidates for next generation photovoltaics. This is due to their outstanding optical and electrical properties which provide large optical cross sections while simultaneously decoupling the photon absorption and charge carrier extraction length scales. These effects relax the requirements for both the minority carrier diffusion length and the amount of semiconductor needed. Metal-semiconductor core-shell nanowires have previously been predicted to show even better optical absorption than solid semiconductor nanowires and offer the additional advantage of a local metal core contact. Here, we fabricate and analyze such a geometry using a single Au-$Cu_2O$ core-shell nanowire photovoltaic cell as a model system. Spatially resolved photocurrent maps reveal that although the minority carrier diffusion length in the $Cu_2O$ shell is less than 1 $\mu$m, the radial contact geometry with the incorporated metal electrode still allows for photogenerated carrier collection along an entire nanowire. Current-voltage measurements yield an open-circuit voltage of 600 mV under laser illumination and a dark diode turn-on voltage of 1 V. This study suggests the metal-semiconductor core-shell nanowire concept could be extended to low-cost, large-scale photovoltaic devices, utilizing for example, metal nanowire electrode grids coated with epitaxially grown semiconductor shells.  [http://dx.doi.org/10.1063/1.4905652]

Photovoltaics provide electricity in a clean, sustainable, and often decentralized way by utilizing an abundant and virtually unlimited source of primary energy: the sun. Wafer-based silicon solar cells are the main driver of increased installations, which reached a global cumulative installed photovoltaic capacity of 137 GW.[1] Other technologies are being pursued that can either lower the overall fabrication costs or increase the conversion efficiency when compared to silicon solar cells.[2] $Cu_2O$ thin film solar cells, for example, are made from abundant, non-toxic, and small amounts of material and can potentially reach power conversion efficiencies of up to 20%.[3] With appropriate surface passivation, thin film solar cells can even reach higher open-circuit voltage ($V_{oc}$) values than their bulk counter parts due to shorter charge carrier extraction paths and hence reduced bulk recombination.[4] Furthermore, when combined with silicon as the bottom absorber ($E_g \sim 1.1$ eV), $Cu_2O$ is an excellent candidate for the top absorber in a high efficiency multijunction solar cell because its band gap ($E_g \sim 2$ eV) is close to ideal (1.7–2.0 eV).[5–7]

Recently, several groups have focused on the interface properties of $Cu_2O$ and were able to increase the $V_{oc}$ up to 1.2 V by using interfacial layers, such as $Ga_2O_3$ and ZnO, combined with transparent conductive oxides (TCOs) as top contacts for $Cu_2O$ thin-film solar cells.[8–18] Light concentration offers another important way to increase the maximum achievable $V_{oc}$, and thereby the conversion efficiency.[19] Conventional triple junction solar cells typically use macroscopic external optics to provide this concentration effect and increase the efficiency, but nanostructures can inherently concentrate light via optical resonances.[20–23] These and other effects are motivating work on next generation high-efficiency photovoltaics, with semiconductor nanowires being among the most promising candidates.[23–26]

Here, we utilize a metal-semiconductor core-shell geometry to fabricate a single horizontally aligned Au-$Cu_2O$ nanowire photovoltaic cell. Such a structure has several potential advantages. The thin semiconductor shell in direct vicinity of the metal core electrode allows for facile extraction of photogenerated carriers, even in materials with short minority carrier diffusion lengths. The radial core-shell geometry has already proven useful in semiconductor nanowire photovoltaics, and we expect even better charge carrier extraction in our geometry where photocarriers are injected into a metal immediately.[27–30] Another previously demonstrated advantage of semiconductor nanowires is their high absorption cross section, which can exceed the geometrical one.[22,23,31] The metal-semiconductor core-shell structure can lead to even higher absorption, while further reducing the amount of semiconductor.[32] Several research groups have already utilized metal-semiconductor core-shell nanospheres or rods for plasmon mediated charge carrier dynamics for photovoltaics and photocatalysis. In these examples, however, semiconductor materials were not used for the visible light absorption or materials were suspended completely in solution.[33–39] Here, we fabricate and test a single metal-semiconductor core-shell nanowire photovoltaic cell, utilizing Au for the core and $Cu_2O$ for the shell.

To fabricate the core-shell nanowires, we followed a procedure developed by Sciacca *et al.* for solution-based synthesis of metal (Ag, Au, or Cu) core $Cu_2O$ shell nanowires.[40] The metal nanowires were synthesized using the polyol process and subsequently coated with a $Cu_2O$ shell at room temperature in aqueous solution adapting a protocol

[a)]Electronic mail: garnett@amolf.nl

 

originally developed for core-shell nanoparticles.[41,42] This specific $Cu_2O$ synthesis route was chosen over other methods to produce $Cu_2O$ nanowires, because it allowed for epitaxial growth on metal nanowires suspended in solution.[43,44] Photoluminescence (PL) measurements showed a peak near 1.9 eV, similar to what has been observed in pure-phase, bulk $Cu_2O$.[40,45]

Figure 1 shows a schematic of a single nanowire photovoltaic cell illuminated by a laser beam. As can be seen in the drawing, the $Cu_2O$ shell has two contacts: one that collects photogenerated holes and one that is selective for photogenerated electrons. One simple and effective method for inducing this carrier selectivity is to use metal contacts with different work functions such that one metal makes an Ohmic contact to the $Cu_2O$ and the other a Schottky junction.[46] Here, we have chosen Au as the metal nanowire core because it has a large work function (~5.4 eV; similar to that of $Cu_2O$) and makes an Ohmic contact to $Cu_2O$. Furthermore, Au has a high chemical stability, low lattice mismatch with $Cu_2O$ (~4%), and a simple nanowire synthesis route.[40,47–50] As the Schottky contact, we have chosen Ti, which has a low work function (~4.3 eV), excellent adhesion to many materials and a stable surface oxide.[51] As reported in previous literature, it is possible that a redox reaction under the Ti contact converts the $Cu_2O$ to $TiO_2$ and Cu at the interface. This modified interface still results in charge carrier separation and extraction, but it does lower the maximum achievable $V_{oc}$ value.[52] We would expect better performance if the contact geometry was reversed, allowing for a Schottky junction along the whole length of the metal core, but such a low work function metal-semiconductor core-shell structure has not been synthesized so far.[40] A more detailed discussion about the influence of the interfaces and the effect of the Schottky junction can be found in the conclusions.

In the current work, we have examined two different Schottky contact geometries: one where a Ti electrode only contacts one end of the nanowire and the other where a thin (~10 nm) layer of Ti is coated along nearly the entire length of the nanowire (Figure 1). By comparing the photocurrent maps in these two geometries, we can directly visualize the effect of local contacts on charge separation and carrier collection efficiency.

To fabricate such samples, we started with $Si_3N_4$ covered Si substrates with evaporated Au electrodes. The core-shell nanowires were contacted using electron beam lithography and metal evaporation. The optical characterization was conducted with a tunable laser source in the range of 410 nm–750 nm. The light was focused through an objective lens to a spot size of ~1 $\mu$m onto the electrically connected single nanowire photovoltaic cells. The details of the device fabrication and characterization can be found in the supplementary material.[67]

Figure 2(a) shows a scanning electron microscope (SEM) image of a typical single nanowire photovoltaic cell (marked by a red arrow). The reflection map in Figure 2(b) shows the diagonal orientation relative to the parallel contact pads. Figure 2(c) shows photocurrent generation of up to 300 pA under 42 $\mu$W laser illumination at $\lambda = 410$ nm. The overlap with the SEM image in Figure 2(d) reveals that charge carrier collection only occurs near the Ti contact finger, where the Schottky junction induces a built-in electric field, such that the minority charge carriers do not have to travel long distances to get extracted. Due to the optically thick Ti contact, we do not expect any substantial contribution to the photocurrent from the $Cu_2O$ regions under the contact.

This photocurrent collection localized only close to the Ti contact suggests that the minority carrier diffusion length is less than or equal to the beam spot size of ~1 $\mu$m, consistent with reported values for $Cu_2O$ synthesized by

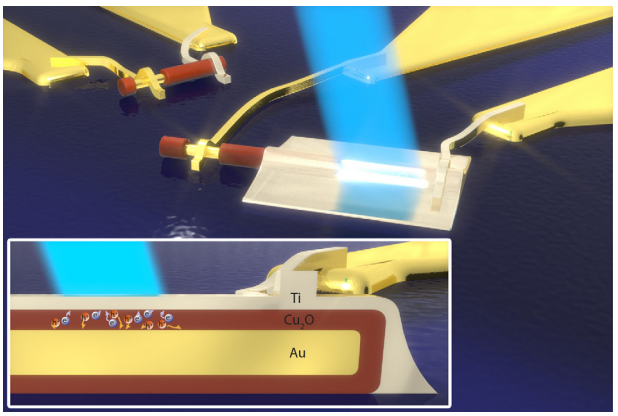


FIG. 1. Schematic drawing of the single metal-semiconductor core-shell nanowire photovoltaic cell geometry. Two devices are electrically connected to electrodes, and a laser beam (bright blue) is incident on one of them. The Au electrode contacts the Au core while a Ti electrode contacts the $Cu_2O$ shell (red) only at the end (top left) or along most of the length via an additional thin Ti pad (center). The inset shows a cross section of the device geometry. The incident light creates electron-hole pairs ($e^-$, $h^+$), which are extracted via the shell and the core, respectively.

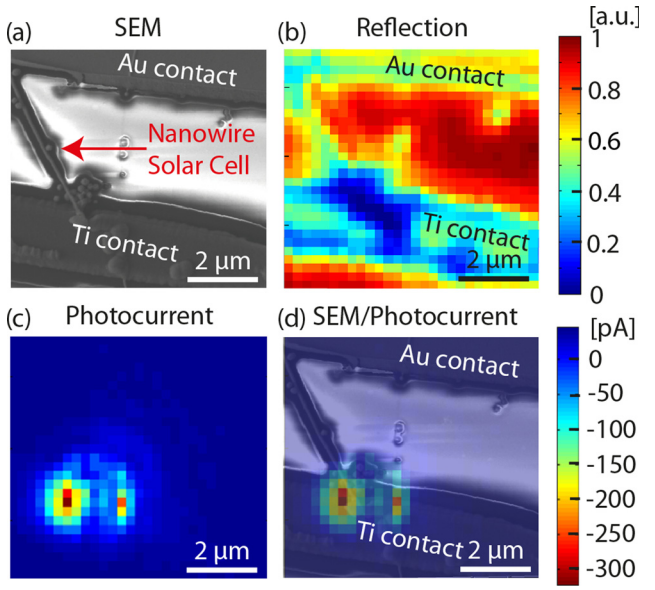


FIG. 2. Metal-semiconductor core-shell nanowire photovoltaic cell with axial charge carrier collection. (a) SEM image of a nanowire (red arrow) connected between Ti and Au contacts. (b) Optical reflection image. (c) Photocurrent map with an incident laser power of 42 $\mu$W, polarization perpendicular to the nanowire axis, a spot size of 1 $\mu$m, and illumination wavelength of 410 nm. (d) Overlay of the photocurrent map and SEM image, clearly showing the local photocurrent collection at the Ti contact.

different methods.[53,54] Despite the excellent crystallinity and epitaxial shell growth in these core-shell nanowires, the high surface and contact areas could lead to even shorter minority carrier diffusion lengths, as these are known to be sources of increased non-radiative recombination in bulk solar cells.[46] Future studies involving thin interfacial spacing layers and surface passivation are needed to quantify the importance of these effects, and our single core-shell nanowire geometry provides a perfect platform for such studies.

To probe directly the importance of the radial built-in field and carrier collection mechanism, we have compared the above results to the case where a 10 nm thin Ti pad covers approximately 2/3 of the nanowire (Figure 3). This arrangement is closer to a realistic large-scale device, where the whole nanowire would be covered with an additional contact (either a transparent conductive oxide or a continuous thick metal layer with illumination through a transparent substrate). Figure 3(a) shows an SEM image of the device, with a Ti pad on top of the nanowire, which is connected between a Ti contact and an Au contact. Figure 3(b) shows the reflection image and Figure 3(c) the respective photocurrent map under 7 $\mu$W laser illumination at $\lambda = 410$ nm, which reveals photocurrent collection from an extended elongated area. The overlay of the SEM and the photocurrent map in Figure 3(d) clearly demonstrates photocurrent collection from the nanowire along the entire length covered by the Ti pad.

This supports the idea that charge carriers generated by light passing through the 10 nm Ti pad can be separated and collected at the metal core and the Ti top contact. The maximum photocurrent is around 25 times smaller than in the axial collection case shown in Figure 2, which can be attributed to the reduction in incident power from 42 to 7 $\mu$W and the substantially reduced absorption in the wire due to the Ti pad. The responsivity (photocurrent after background subtraction divided by the incident laser power) is only lowered by a factor of four by the Ti pad. These results prove the utility of this concept: photocurrent collection can take place along the whole length of the nanowire, even with materials that have very short minority carrier diffusion lengths.

To investigate the core-shell nanowire spectral response, we map the responsivity under 410 nm, 520 nm, 620 nm, and 700 nm laser illumination (Figures 4(c)–4(f), respectively). The polarization was perpendicular to the nanowire axis for all measurements, which is the polarization that supports plasmon resonances. In the other polarization, we observed weaker currents. Currently, we cannot distinguish between charge carrier generation due to band to band absorption in the $Cu_2O$ and plasmon mediated transfer mechanisms, such as resonance energy transfer, direct energy transfer, and hot electron carrier injection.[33,55–59]

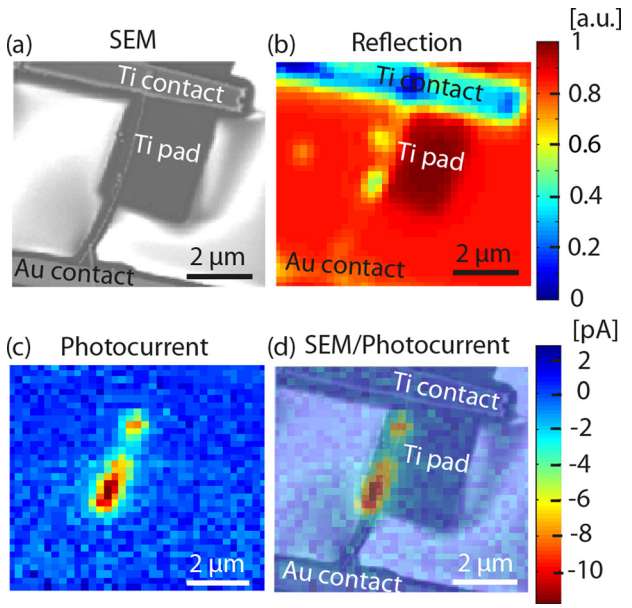


FIG. 3. Metal-semiconductor core-shell nanowire photovoltaic cell with radial charge carrier collection. (a) SEM image of a nanowire connected between Ti and Au contacts and partially covered by a 10 nm thin Ti pad. (b) Reflection map. (c) Photocurrent map with an incident laser power of 7 $\mu$W, polarization perpendicular to the nanowire axis, a spot size of 1 $\mu$m, and illumination wavelength of 410 nm. (d) Overlay of photocurrent map and SEM image, clearly showing the photocurrent collection from the Ti covered part of the nanowire.

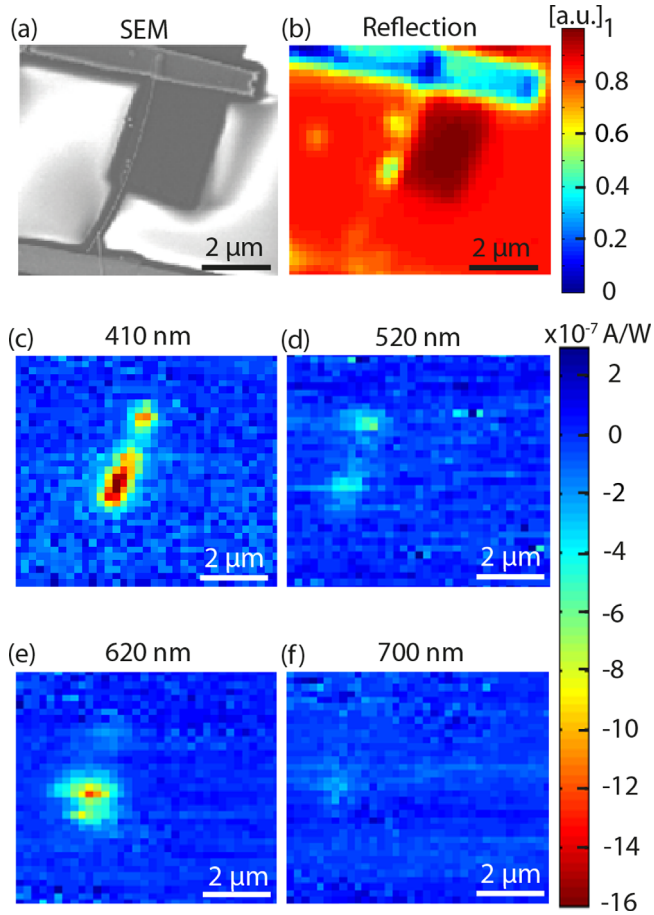


FIG. 4. Spectral response of a metal-semiconductor core-shell nanowire photovoltaic cell. (a) SEM image of the same nanowire solar cell shown in Figure 3. (b) Reflection map at 410 nm showing the contact pad and contact fingers. (c)–(f) Responsivity maps at laser wavelengths of (c) 410 nm, (d) 520 nm, (e) 620 nm, and (f) 700 nm. The responsivity was obtained by first subtracting the background values and subsequently dividing by the incident laser power, to facilitate comparison. In all cases, the laser polarization was perpendicular to the nanowire axis. The spatial shift of the photocurrent with increasing wavelengths is due to chromatic aberration of the objective lens and drift in the mechanical stage.

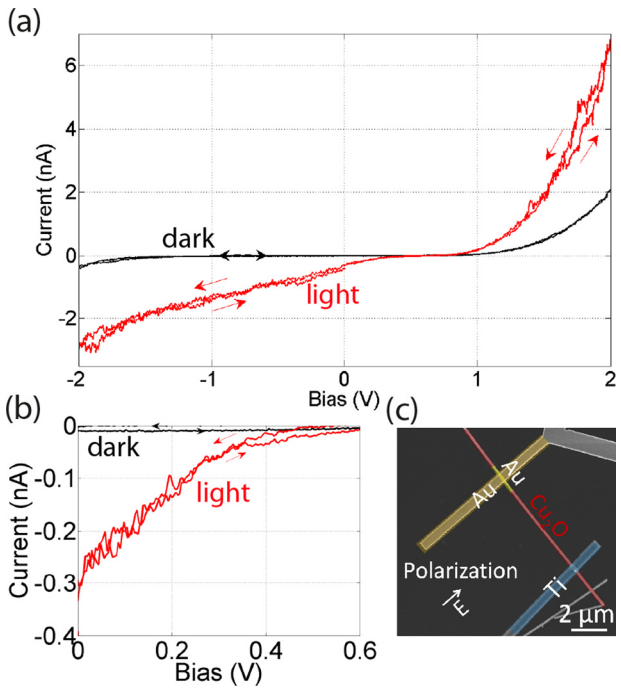


FIG. 5. (a) Current-voltage behavior of a single Au-$Cu_2O$ core-shell nanowire photovoltaic cell in the dark (black line) and under laser illumination at 410 nm with a power of 42 $\mu$W and polarization perpendicular to the nanowire axis (red). (b) Magnified view of the region 0 V–0.6 V of the I-V curves. (c) SEM image with color overlay of a connected nanowire.

The strong reduction in photocurrent for $\lambda = 700$ nm is consistent with the literature value of the optical band gap (1.95 eV or 635 nm) and our own single nanowire PL measurements.[40,60] However, absorption in the Ti pad as well as variations in the optical resonances must be taken into account to quantitatively explain the observed results.

Finally, we show single nanowire current-voltage (I-V) measurements in the dark and under laser illumination (Figure 5). This nanowire device, which did not contain an extended Ti pad (Figure 5(c)), showed clear rectification behavior with a turn on voltage of $\sim$1 V in the dark. Under laser illumination with 42 $\mu$W power at 410 nm, an $I_{sc}$ of $-300$ pA and a $V_{oc}$ of 600 mV were observed. These results clearly demonstrate that single metal-semiconductor core-shell nanowires function as photovoltaic cells. The photocurrent increases at higher reverse voltages and reaches reverse break down before saturating. We attribute this slope to higher photogenerated carrier collection efficiency at larger reverse bias voltages due to an increased depletion region. Furthermore, we observe a substantial charge carrier extraction barrier and hence S-shaped I-V curve, which is a well-known phenomena that can be attributed to accumulated space charges at the material interfaces or a non-ideal Ohmic contact.[61–64] This observation can be explained by the non-optimized metal semiconductor interfaces, which are likely to induce recombination-active trap states and accumulated space charges. We note that the photocurrent under the AM 1.5G spectrum was below the detection limit ($\sim$1 pA) of the source measure unit used and therefore did not allow the measurement of our devices under the full solar spectrum. The low photocurrent can partially be explained by the localized Schottky region close to the optically thick Ti contact, which is mostly inaccessible for the incident light. Only a small fraction at the edge of the contact can contribute to the photocurrent.

In conclusion, we have realized a single metal-semiconductor core-shell nanowire photovoltaic cell. We measured photocurrent maps on individual Au-$Cu_2O$ core-shell nanowires, showing charge carrier collection via a Schottky contact on the surface, with the metal core being utilized as an Ohmic contact. The spectral response is consistent with a band gap of $\sim$2 eV. We show that a $V_{oc}$ of 0.6 V and $I_{sc}$ of 300 pA can be achieved without any detailed contact optimization, while much higher values can be expected by incorporating appropriate interfacial layers, as already demonstrated not only with $Cu_2O$ but also other material systems that use ultrathin absorber layers such as organics and hybrid perovskites.[8,65,66] By depositing a thin (10 nm) Ti layer over the wire, we clearly demonstrate that two conductive radial metal contacts allow for improved photogenerated carrier collection in semiconductors with minority carrier diffusion lengths $<1$ $\mu$m.

While the limitations discussed above explain the overall low photovoltaic performance of our devices, they do not present insurmountable obstacles on the way to high efficiency metal-semiconductor core-shell nanowire solar cells. In fact, the strong dependence of nanostructured solar cells on surface and interface properties presents an opportunity to study these effects in a highly controlled system where changes at the semiconductor surface or metal-semiconductor interface can be directly measured in the photovoltaic response of the device. Any new insights gained here can be applied to existing thin-film technology where the metal-semiconductor contact is also a crucial source of loss but more difficult to isolate and study. Furthermore, we note that the metal-semiconductor core-shell nanowire geometry is not limited to the materials used for this proof-of-concept study. An ideal structure would employ low cost metals with appropriate interfacial layers, replacing Au and Ti. Therefore, we propose metal-semiconductor core-shell nanowire photovoltaics as both an ideal platform for fundamental interfacial studies as well as a promising geometry for high efficiency solar cells made from materials with very short minority carrier diffusion lengths.

We are thankful to Duncan Verheijde, Henk-Jan Boluijt, and Wim Brouwer for help with the design and construction of the electrical measurement components, Marco Seynen for software engineering, Joop Rovekamp for help with wire bonding, Henk-Jan Boluijt for creating the schematic picture in Figure 1, and Jorik van de Groep for a careful reading of the manuscript. Furthermore, we would like to acknowledge support from the Light Management in New Photovoltaic Materials (LMPV) center at AMOLF. This work is part of the research program of the Foundation for Fundamental Research on Matter (FOM), which is part of the Netherlands Organization for Scientific Research (NWO). The research leading to these results has received funding from the European Research Council under the European Union's Seventh Framework Programme (FP/2007-2013)/ERC Grant Agreement No. 337328, "NanoEnabledPV."

[1]European Photovoltaic Industry Association, Market Report 2013 (2013).
[2]M. A. Green, Prog. Photovoltaics: Res. Appl. **9**, 123 (2001).
[3]B. K. Meyer, A. Polity, D. Reppin, M. Becker, P. Hering, P. J. Klar, T. Sander, C. Reindl, J. Benz, M. Eickhoff, C. Heiliger, M. Heinemann, J. Bläsing, A. Krost, S. Shokovets, C. Müller, and C. Ronning, Phys. Status Solidi B **249**, 1487 (2012).
[4]M. Green, IEEE Trans. Electron Devices **31**, 671 (1984).
[5]F. Meillaud, A. Shah, C. Droz, E. Vallat-Sauvain, and C. Miazza, Sol. Energy Mater. Sol. Cells **90**, 2952 (2006).
[6]F. Dimroth, M. Grave, P. Beutel, U. Fiedeler, C. Karcher, T. N. D. Tibbits, E. Oliva, G. Siefer, M. Schachtner, A. Wekkeli, A. W. Bett, R. Krause, M. Piccin, N. Blanc, C. Drazek, E. Guiot, B. Ghyselen, T. Salvetat, A. Tauzin, T. Signamarcheix, A. Dobrich, T. Hannappel, and K. Schwarzburg, Prog. Photovoltaics: Res. Appl. **22**, 277 (2014).
[7]Z. M. Beiley and M. D. McGehee, Energy Environ. Sci. **5**, 9173 (2012).
[8]Y. S. Lee, D. Chua, R. E. Brandt, S. C. Siah, J. V. Li, J. P. Mailoa, S. W. Lee, R. G. Gordon, and T. Buonassisi, Adv. Mater. **26**, 4704 (2014).
[9]T. Minami, Y. Nishi, and T. Miyata, Appl. Phys. Express **6**, 044101 (2013).
[10]Y. S. Lee, J. Heo, M. T. Winkler, S. C. Siah, S. B. Kim, R. G. Gordon, and T. Buonassisi, J. Mater. Chem. A **1**, 15416 (2013).
[11]S. W. Lee, Y. S. Lee, J. Heo, S. C. Siah, D. Chua, R. E. Brandt, S. B. Kim, J. P. Mailoa, T. Buonassisi, and R. G. Gordon, Adv. Energy Mater. **4**, 1301916 (2014).
[12]C. Xiang, G. M. Kimball, R. L. Grimm, B. S. Brunschwig, H. A. Atwater, and N. S. Lewis, Energy Environ. Sci. **4**, 1311 (2011).
[13]K. P. Hering, R. E. Brandt, B. Kramm, T. Buonassisi, and B. K. Meyer, Energy Procedia **44**, 32 (2014).
[14]T. Oku, T. Yamada, K. Fujimoto, and T. Akiyama, Coatings **4**, 203 (2014).
[15]C.-C. Chen, L.-C. Chen, and Y.-H. Lee, Adv. Condens. Matter Phys. **2012**, 129139.
[16]A. T. Marin, D. Muñoz-Rojas, D. C. Iza, T. Gershon, K. P. Musselman, and J. L. MacManus-Driscoll, Adv. Funct. Mater. **23**, 3413 (2013).
[17]T. S. Gershon, A. K. Sigdel, A. T. Marin, M. F. A. M. van Hest, D. S. Ginley, R. H. Friend, J. L. MacManus-Driscoll, and J. J. Berry, Thin Solid Films **536**, 280 (2013).
[18]T. Minami, Y. Nishi, T. Miyata, and J. Nomoto, Appl. Phys. Express **4**, 062301 (2011).
[19]W. Shockley and H. J. Queisser, J. Appl. Phys. **32**, 510 (1961).
[20]Z. I. Alferov, V. M. Andreev, and V. D. Rumyantsev, *Concentrator Photovoltaics*, Springer Series in Optical Sciences, edited by A. Luque and V. Andreev (Springer, 2007), pp. 151–174.
[21]H. A. Atwater and A. Polman, Nat. Mater. **9**, 205 (2010).
[22]P. Krogstrup, H. I. Jørgensen, M. Heiss, O. Demichel, J. V. Holm, M. Aagesen, J. Nygard, and A. Fontcuberta i Morral, Nat. Photonics **7**, 306 (2013).
[23]J. Wallentin, N. Anttu, D. Asoli, M. Huffman, I. Aberg, M. H. Magnusson, G. Siefer, P. Fuss-Kailuweit, F. Dimroth, B. Witzigmann, H. Q. Xu, L. Samuelson, K. Deppert, and M. T. Borgström, Science **339**, 1057 (2013).
[24]E. C. Garnett, M. L. Brongersma, Y. Cui, and M. D. McGehee, Annu. Rev. Mater. Res. **41**, 269 (2011).
[25]T. J. Kempa, R. W. Day, S.-K. Kim, H.-G. Park, and C. M. Lieber, Energy Environ. Sci. **6**, 719 (2013).
[26]M. L. Brongersma, Y. Cui, and S. Fan, Nat. Mater. **13**, 451 (2014).
[27]Z. Fan, H. Razavi, J. Do, A. Moriwaki, O. Ergen, Y.-L. Chueh, P. W. Leu, J. C. Ho, T. Takahashi, L. A. Reichertz, S. Neale, K. Yu, M. Wu, J. W. Ager, and A. Javey, Nat. Mater. **8**, 648 (2009).
[28]M. Law, L. E. Greene, J. C. Johnson, R. Saykally, and P. Yang, Nat. Mater. **4**, 455 (2005).
[29]B. Tian, X. Zheng, T. J. Kempa, Y. Fang, N. Yu, G. Yu, J. Huang, and C. M. Lieber, Nature **449**, 885 (2007).
[30]J. M. Spurgeon, H. A. Atwater, and N. S. Lewis, J. Phys. Chem. C **112**, 6186 (2008).
[31]L. Cao, J. S. White, J.-S. Park, J. A. Schuller, B. M. Clemens, and M. L. Brongersma, Nat. Mater. **8**, 643 (2009).
[32]S. A. Mann and E. C. Garnett, Nano Lett. **13**, 3173 (2013).
[33]S. Mubeen, J. Lee, N. Singh, S. Krämer, G. D. Stucky, and M. Moskovits, Nat. Nanotechnol. **8**, 247 (2013).
[34]F. P. Garcia de Arquer, A. Mihi, D. Kufer, and G. Konstantatos, ACS Nano **7**, 3581 (2013).
[35]Y. Nishijima, K. Ueno, Y. Yokota, K. Murakoshi, and H. Misawa, J. Phys. Chem. Lett. **1**, 2031 (2010).
[36]Y. Takahashi and T. Tatsuma, Appl. Phys. Lett. **99**, 182110 (2011).
[37]Y. K. Lee, C. H. Jung, J. Park, H. Seo, G. A. Somorjai, and J. Y. Park, Nano Lett. **11**, 4251 (2011).
[38]P. Reineck, G. P. Lee, D. Brick, M. Karg, P. Mulvaney, and U. Bach, Adv. Mater. **24**, 4750 (2012).
[39]S. Mubeen, J. Lee, W.-R. Lee, N. Singh, G. D. Stucky, and M. Moskovits, ACS Nano **8**, 6066 (2014).
[40]B. Sciacca, S. A. Mann, F. D. Tichelaar, H. W. Zandbergen, M. A. van Huis, and E. C. Garnett, Nano Lett. **14**, 5891 (2014).
[41]B. Wiley, Y. Sun, and Y. Xia, Acc. Chem. Res. **40**, 1067 (2007).
[42]C.-H. Kuo, T.-E. Hua, and M. H. Huang, J. Am. Chem. Soc. **131**, 17871 (2009).
[43]S. Hacialioglu, F. Meng, and S. Jin, Chem. Commun. **48**, 1174 (2012).
[44]S. Brittman, Y. Yoo, N. P. Dasgupta, S. Kim, B. Kim, and P. Yang, Nano Lett. **14**, 4665 (2014).
[45]J. I. Jang, *Cuprous Oxide (Cu2O): A Unique System Hosting Various Excitonic Matter and Exhibiting Large Third-Order Nonlinear Optical Responses* (InTech, Rijeka, 2011), pp. 137–164.
[46]P. Wuerfel, *Physics of Solar Cells*, 2nd ed. (Wiley-VCH, Weinheim, 2009), p. 150.
[47]E. E. Huber, Appl. Phys. Lett. **8**, 169 (1966).
[48]*Cuprous Oxide (Cu2O) Crystal Structure, Lattice Parameters*, edited by O. Madelung, U. Roessler, and M. Schulz (Springer, Berlin, Heidelberg, 1998), pp. 1–3.
[49]M. B. Brodsky, J. Phys., Colloq. **45**, C5 (1984).
[50]J.-D. Kwon, S.-H. Kwon, T.-H. Jung, K.-S. Nam, K.-B. Chung, D.-H. Kim, and J.-S. Park, Appl. Surf. Sci. **285**, 373 (2013).
[51]*CRC Handbook of Chemistry and Physics*, 85th ed., edited by D. R. Linde (CRC Press, New York, 2005).
[52]L. C. Olsen, R. C. Bohara, and M. W. Urie, Appl. Phys. Lett. **34**, 47 (1979).
[53]K. P. Musselman, Y. Ievskaya, and J. L. MacManus-Driscoll, Appl. Phys. Lett. **101**, 253503 (2012).
[54]Y. Liu, H. K. Turley, J. R. Tumbleston, E. T. Samulski, and R. Lopez, Appl. Phys. Lett. **98**, 162105 (2011).
[55]S. K. Cushing, J. Li, F. Meng, T. R. Senty, S. Suri, M. Zhi, M. Li, A. D. Bristow, and N. Wu, J. Am. Chem. Soc. **134**, 15033 (2012).
[56]P. Fan, Z. Yu, S. Fan, and M. L. Brongersma, Nat. Mater. **13**, 471 (2014).
[57]P. Fan, K. C. Y. Huang, L. Cao, and M. L. Brongersma, Nano Lett. **13**, 392 (2013).
[58]P. Fan, U. K. Chettiar, L. Cao, F. Afshinmanesh, N. Engheta, and M. L. Brongersma, Nat. Photonics **6**, 380 (2012).
[59]S. Brittman, H. Gao, E. C. Garnett, and P. Yang, Nano Lett. **11**, 5189 (2011).
[60]F. C. Akkari and M. Kanzari, Phys. Status Solidi A **207**, 1647 (2010).
[61]A. Wagenpfahl, D. Rauh, M. Binder, C. Deibel, and V. Dyakonov, Phys. Rev. B **82**, 115306 (2010).
[62]M. Zhang, H. Wang, and C. W. Tang, Appl. Phys. Lett. **99**, 213506 (2011).
[63]R. Saive, C. Mueller, J. Schinke, R. Lovrincic, and W. Kowalsky, Appl. Phys. Lett. **103**, 243303 (2013).
[64]A. Kumar, S. Sista, and Y. Yang, J. Appl. Phys. **105**, 094512 (2009).
[65]S. Ryu, J. H. Noh, N. J. Jeon, Y. Chan Kim, W. S. Yang, J. Seo, and S. Il Seok, Energy Environ. Sci. **7**, 2614 (2014).
[66]A. W. Hains, J. Liu, A. B. F. Martinson, M. D. Irwin, and T. J. Marks, Adv. Funct. Mater. **20**, 595 (2010).
[67]See supplementary material at http://dx.doi.org/10.1063/1.4905652 for experimental details.